Supplementary Information for:

Large changes in biomass burning over the last millennium inferred from paleoatmospheric ethane in polar ice cores

Melinda R. Nicewonger, Murat Aydin, Michael J. Prather, and Eric S. Saltzman

Corresponding author: Melinda R. Nicewonger

Email: nicewonm@uci.edu

This PDF file includes:

Supplementary text

Figs. S1 to S7 (Figs. S1 through S5 are referenced in the main manuscript)

Tables S1 to S6 (Tables S1 through S3 are referenced in the main manuscript)

References for SI reference citations

Supplementary Information Text

Ice core site characteristics and chronology

Greenland Ice Sheet Project 2 (GISP2): Samples from a dry-drilled (GISP2B, n=6) and a fluid-drilled core (GISP2D, n-butyl acetate used as drill-fluid, n=11) were analyzed for ethane during this project. The accumulation rate at Summit, Greenland (the GISP2 site) is 24 cm y⁻¹ ice equivalent and the mean annual temperature is -31°C (1). Gas ages for GISP2D were calculated by linear interpolation of the GISP2D ice-age scale to our sample depths and subtracting a Δ_{age} (ice age – gas age) of 199 years from the calculated ice ages (2,3). Gas ages for GISP2B were calculated by applying a +5-year offset to the GISP2D ice-age scale and subtracting the same Δ_{age} (4). Uncertainty of the GISP2 gas age is 1%.

West Antarctic Ice Sheet (WAIS) Divide: Samples from a dry-drilled (WDC-05A, n=21) and a fluid drilled core (WDC-06A, mixture of Isopar-K and HCFC-141b used as drill fluid, n=21) were analyzed for ethane. The WDC-05A and 06A ice cores were drilled as part of the WAIS Divide project (5). The gas ages for the WDC-05A samples were calculated by linear interpolation from the nearest depths in the WDC05A-2 ice-age chronology and subtracting a Δ_{age} of 208 years (6). The WDC-06A samples were dated by linear interpolation from the nearest depths in the WD2014 ice-age chronology (7,8), then subtracting the same Δ_{age} to calculate a gas age for each WDC-06A sample. Uncertainty on the mean age for WDC-05A and WDC-06A is 1% and 0.5%, respectively.

South Pole Ice Core (SPC14): We analyzed samples from the fluid-drilled SPC14 core (n=11, Estisol 140 as drill fluid). The SPC14 core was drilled 2.7 km from the South Pole Station during 2014-2016 to a final depth of 1751 m. The mean accumulation rate at the SPC14 site is 8 cm y⁻¹ ice equivalent and the mean annual temperature is -49°C (9). Samples were dated using methane

ties to the WD2014 ice-age chronology (7,8). A Δ_{age} of 1000 years is used to calculate a gas-age for each sample. Uncertainty on the mean age is roughly \pm 30 years.

Ice core quality control

In addition to ethane, the ice core samples were simultaneously analyzed for CFC-12 using methods described previously (4,10). CFC-12 in the atmosphere prior to the mid-20th century was negligible and therefore bubbles trapped in the ice core samples prior to this period should not contain CFC-12. Four Greenland and two Antarctic samples had CFC-12 greater than 1 pmol mol⁻¹ and were not used in the interpretations presented in this study.

Analytical blanks

 N_2 blanks were conducted after each sample melt to quantify the background (blank) level of ethane in the extraction system. Ethane mixing ratios in the samples (X_{ethane}) are calculated as follows:

$$X_{ethane} \text{ (pmol mol}^{-1}) = \frac{m_{sample} - m_{blank}}{m_{air}}$$

where m_{sample} is the amount of ethane measured in the sample (pmol), m_{blank} is the average amount of ethane (pmol) in the post-melt blanks from a series of samples, and m_{air} is the amount of dry air (mol) extracted from the ice core sample.

The analytical blank in the wet extraction system has declined steadily over time. We correct all samples with a mean blank from the most recent analysis conducted in late 2017 (mean blank = 0.03 pmol ethane, n=19). The uncertainty on the blank ($1\sigma = 0.01$ pmol ethane) is included in the total error calculation, which also includes a calibration uncertainty. The mean analytical blank

corresponds to roughly 5% of the total ethane signal (includes the blank) from the Greenland ice core samples and roughly 18% of the total signal from the Antarctic ice core samples.

Methane Box Model

The one box steady state methane model solves the mass balance equations for CH_4 , $^{12}CH_4$ and $^{13}CH_4$ as follows:

$$CH_4 = \frac{\sum sources}{k_{total}} = \frac{geologic + microbial + biomass + biofuel}{(k_{OH} + k_{soil} + k_{strat})}$$

$$^{12}CH_4 = \frac{\sum^{12}CH_4 \text{ sources}}{(k_{OH} + k_{soil} + k_{strat})}$$

$$^{13}CH_{4} = \frac{\sum{}^{13}CH_{4} sources}{(\alpha_{OH}*k_{OH} + \alpha_{soil}*k_{OH} + \alpha_{strat}*k_{strat})}$$

$$\delta^{13}\text{CH}_4 = \left(\left(\frac{(^{13}\text{CH}_4/^{12}\text{CH}_4)_{\text{sample}}}{(^{13}\text{CH}_4/^{12}\text{CH}_4)_{\text{std}}} \right) - 1 \right) * 1000$$

where sources are in units of Tg y⁻¹, and each loss constant (k) is calculated from the total methane loss constant (1/9.5 y⁻¹) by multiplying their respective relative contributions (Table S4) with the total loss. The 13 C/ 12 C standard used is 0.0112372 (11). End member 13 C/ 12 C ratios of various sources (Table S5) were assigned based on Schwietzke et al. (12) and kinetic isotope

effect (α) for the methane loss pathways are given in Table S4. A constant biofuel source of 6 Tg y^{-1} was used in every emission scenario.

Goodness of fit calculation

We calculated a goodness of fit for the emission scenarios that passed the cost function calculation (see main text). The goodness of fit is calculated as:

$$Goodness\ of\ fit_{ethane} = \sqrt{\left(\frac{\left|m_{grn}\ -\ o_{grn}\right|}{o_{grn}}\right)^2\ +\ \left(\frac{\left|m_{ant}\ -\ o_{ant}\right|}{o_{ant}}\right)^2}$$

$$Goodness\ of\ fit_{methane} = \sqrt{\left(\frac{\left|m_{[CH_{4}]} - o_{[CH_{4}]}\right|}{o_{[CH_{4}]}}\right)^{2} + \left(\frac{\left|m_{\delta^{13}CH_{4}} - o_{\delta^{13}CH_{4}}\right|}{\left|\delta^{13}CH_{4_max} - \delta^{13}CH_{4_min}\right|}\right)^{2}}$$

where m stands for the modeled value and o for the observed mean value from the ice core records. The goodness of fit was calculated for the MP and LIA separately and are shown in Figs. S2, S4 and S5. The goodness of fit ranges from 0 to 0.14, with 0 corresponding to a perfect fit to the mean of the ice core records.

UCI ethane calibration

The UCI ethane calibration is an internal laboratory scale based on three primary gas standards (high pressure aluminum cylinders) prepared and maintained in our laboratory (4,14). The accuracy of the ethane gas standards is estimated to be $\pm 5\%$ based on the uncertainties in the volumetric and gravimetric measurements involved and in the purity of the reagent ethane. The precision of the preparation of the primary gas standards can be estimated from the agreement between the calibration curves from individual primary gas standards. One standard deviation of

the calibration curve slopes from three different primary gas standards is 1-2%. This indicates the precision with which the cylinders are prepared and analyzed and supports our estimate of accuracy.

The UCI ethane calibration scale has not been directly compared to the World Meteorological Organization Global Atmospheric Watch (WMO-GAW) ethane standard. However, we routinely analyze air collected by the NOAA GMD HATS program from Cape Grim, Australia and South Pole, Antarctica (https://www.esrl.noaa.gov/gmd/hats/). We can obtain an estimate of how the UCI scale compares to the WMO-GAW ethane standard by comparing our flask measurements to measurements of NOAA GMD Carbon Cycle glass flasks from the same sites analyzed by the Helmig lab at UC Boulder. The Helmig lab's ethane measurements have been audited by WMO-GAW and found to be within ± 5% of the certified standard (15, 16).

The comparison was conducted for Cape Grim (2006-2016) and South Pole (2006-2016) (Fig. S6) using data from https://www.esrl.noaa.gov/gmd/dv/data/. We averaged individual flask measurements from each site to calculate monthly means and standard deviations of ethane levels for NOAA and UCI separately. Quality control was performed on both the NOAA and UCI data by eliminating: 1) data with a non-blank flag indicating quality concerns (NOAA only), 2) monthly data with a relative standard deviation (1σ /mean) >0.2, and 3) monthly data with a mean level >350 pmol mol⁻¹. Two-way (orthogonal) linear regressions (https://www.mathworks.com/matlabcentral/fileexchange/33484-linear-deming-regression) were fit to the monthly mean ethane levels from Cape Grim and South Pole (Fig. S7). The two-way linear regressions yield slopes of 1.04 ± 0.06 (1 standard error) for South Pole and 1.02 ± 0.06 for Cape Grim. The relatively large scatter in the data (with respect to the reported analytical

precisions) can be due to various sampling or sample storage (while inside the flasks) issues arising from the fact that the two laboratories analyze different sets of NOAA flasks filled on different days of the month. The slopes and intercepts of the data comparison from both sites indicate no statistically significant difference between the ethane calibration scales of the two laboratories.

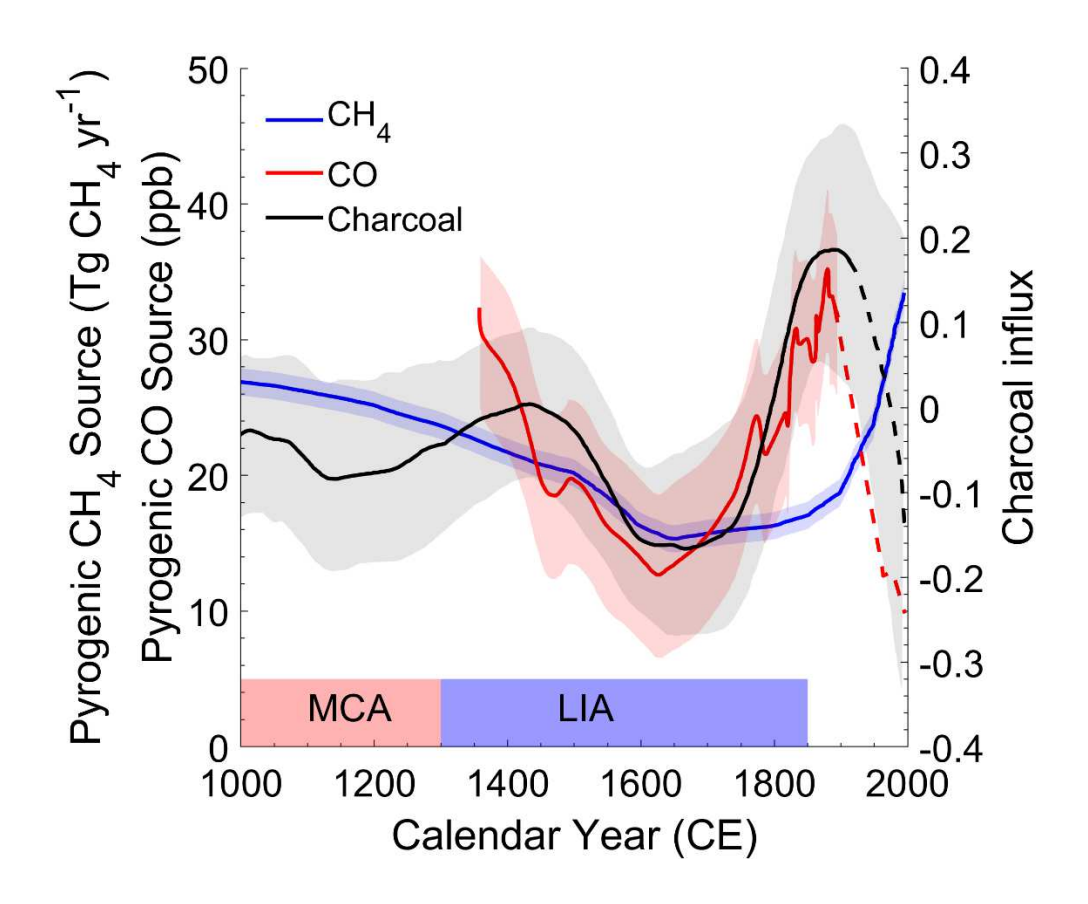


Fig. S1. Previous reconstructions of biomass burning over the past millennium. Shaded regions highlight the timing of the Medieval Climate Anomaly (MCA) and Little Ice Age (LIA). Black: composite of sedimentary charcoal records (17), Blue: pyrogenic methane based on ice core methane and δ^{13} CH₄ in an Antarctic ice core (18), Red: pyrogenic carbon monoxide based on CO, δ^{13} CO and δ^{C18} O measurements in an Antarctic ice core (19).

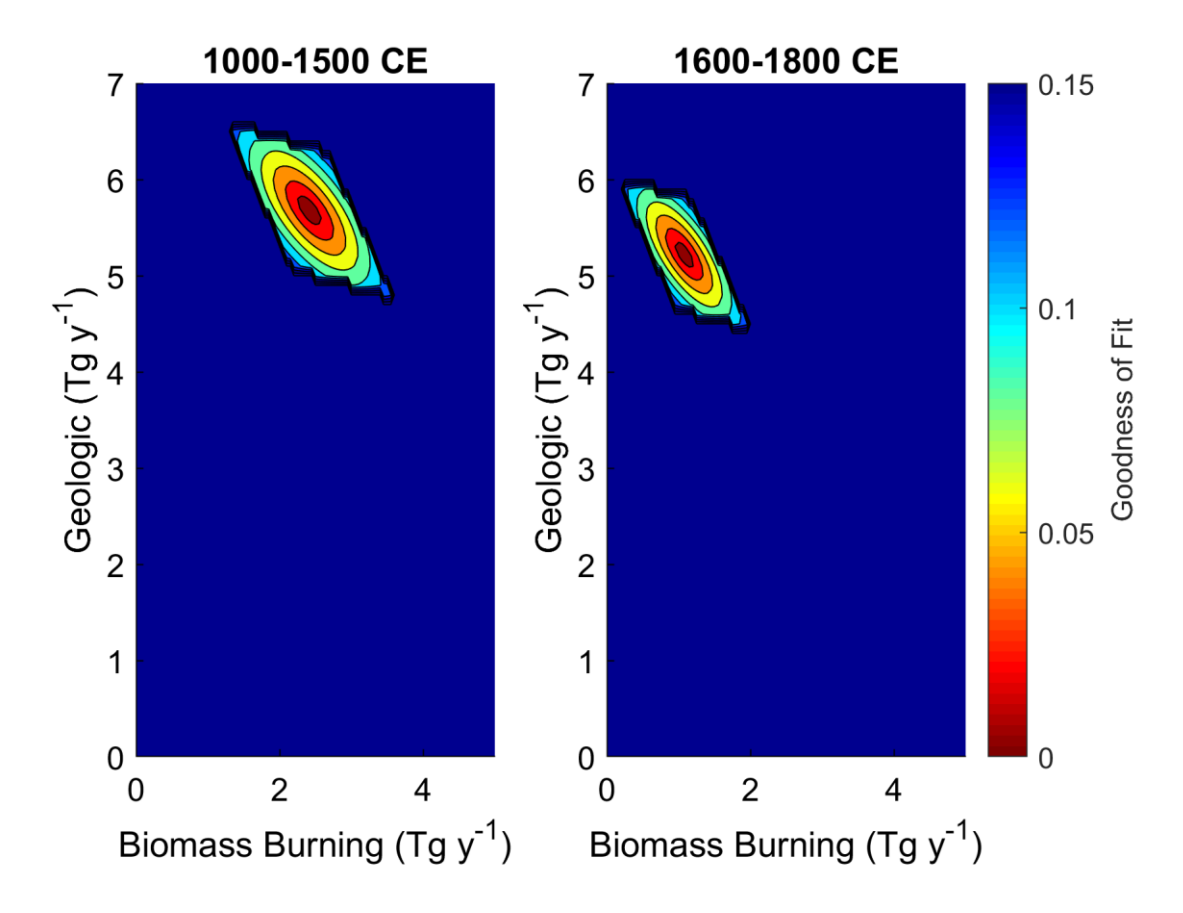


Fig. S2. Modeled ethane geologic and biomass burning emission scenarios for the Medieval Period (1000-1500 CE, left) and the Little Ice Age (1600-1800 CE, right). Contours are of goodness of fit (see SI Appendix text for calculation), with a value of 0 corresponding to a perfect fit to the mean of the ice core records. Emissions are in Tg ethane y⁻¹.

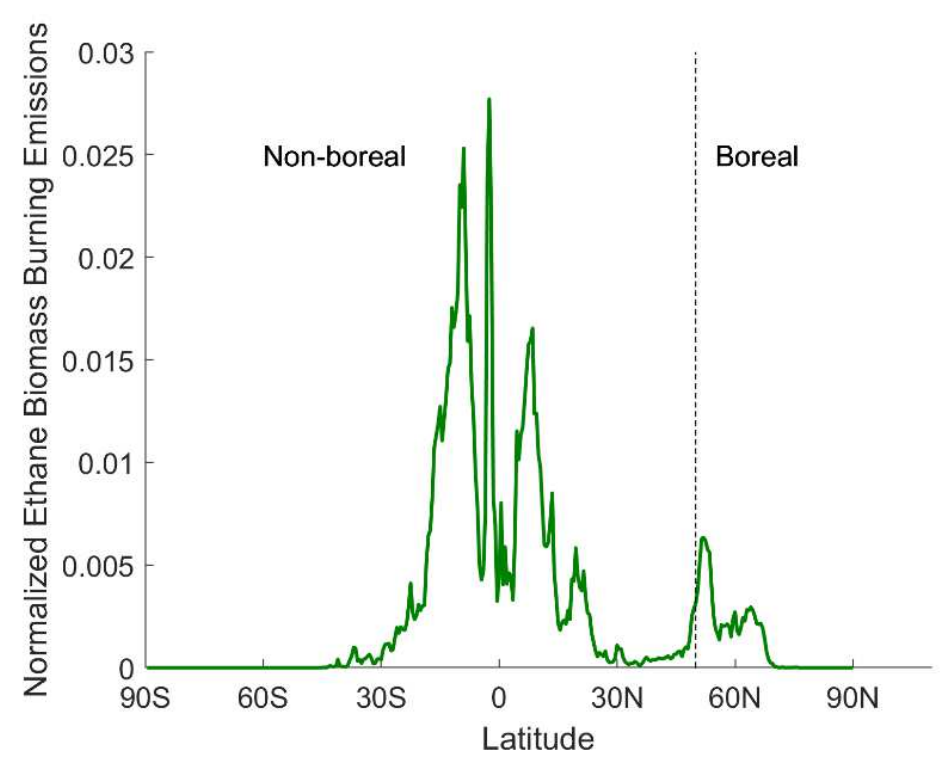


Fig. S3. Global distribution of ethane biomass burning emissions from GFED3.1 (20). Emissions are normalized. The dashed line denotes the non-boreal (50°N to 90°S) and boreal (>50°N) zones used in this study.

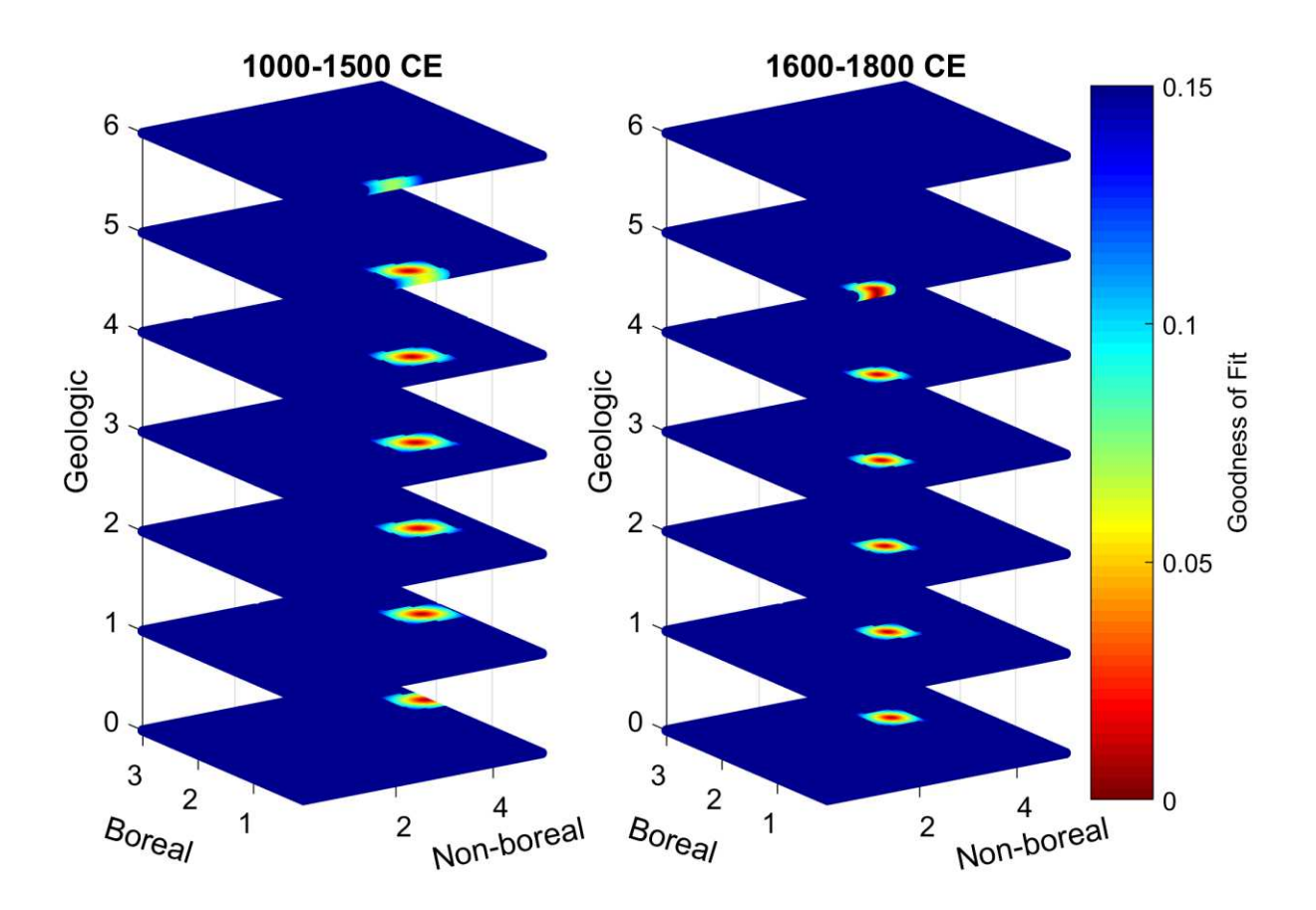


Fig. S4. Modeled ethane boreal and non-boreal biomass burning and geologic emission scenarios for the Medieval Period (1000-1500 CE, left) and Little Ice Age (1600-1800 CE, right). Contours are of goodness of fit (see SI Appendix text for calculation), with a value of 0 corresponding to a perfect fit to the mean of the ice core records. Emissions are in Tg ethane y⁻¹.

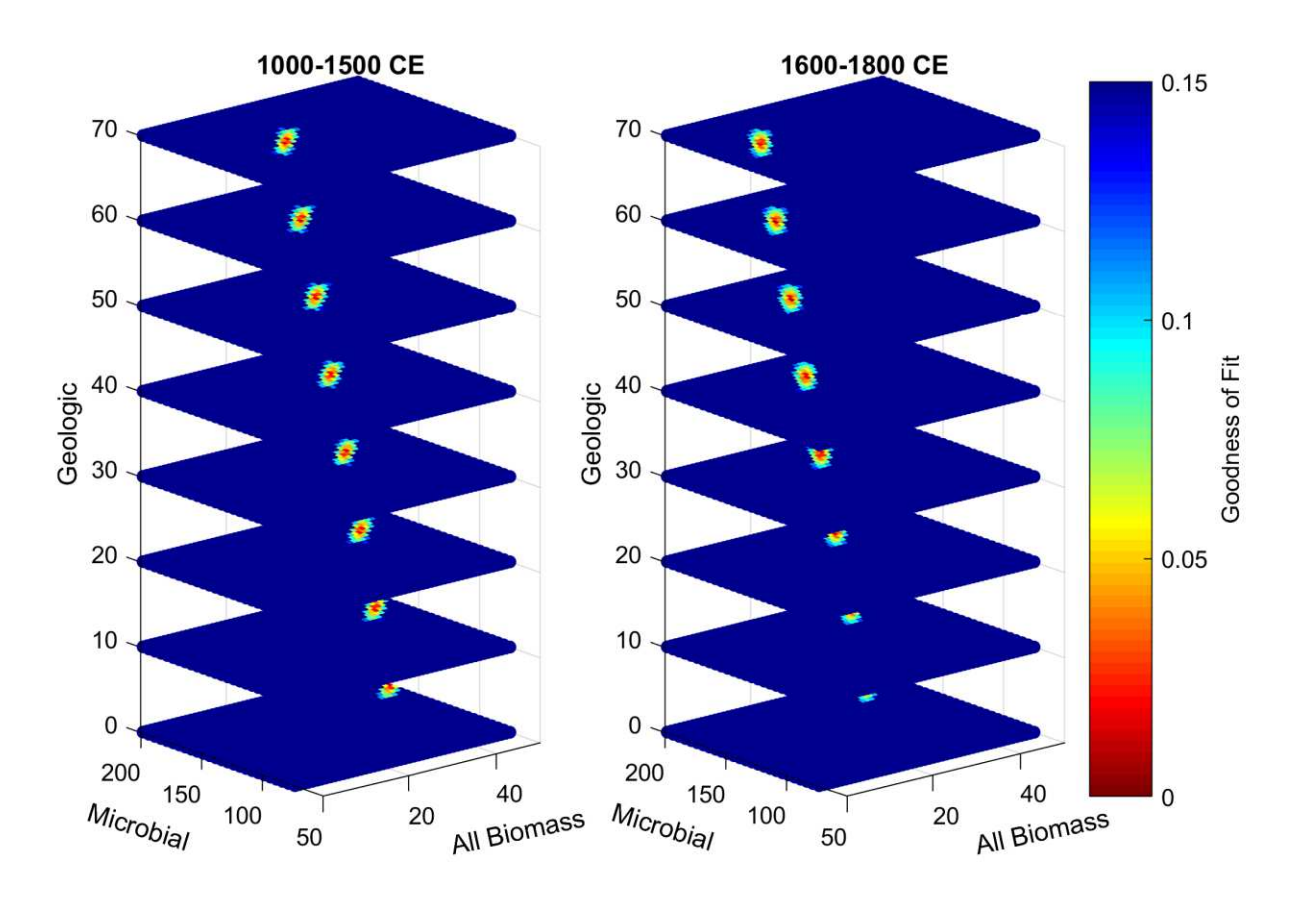


Fig. S5. Modeled methane geologic, microbial, and biomass burning emission scenarios for the Medieval Period (1000-1500 CE, left) and the Little Ice Age (1600-1800 CE, right). Contours are of goodness of fit (see SI Appendix text for calculation), with a value of 0 corresponding to a perfect fit to the mean of the ice core records. Emissions are in Tg methane y⁻¹.

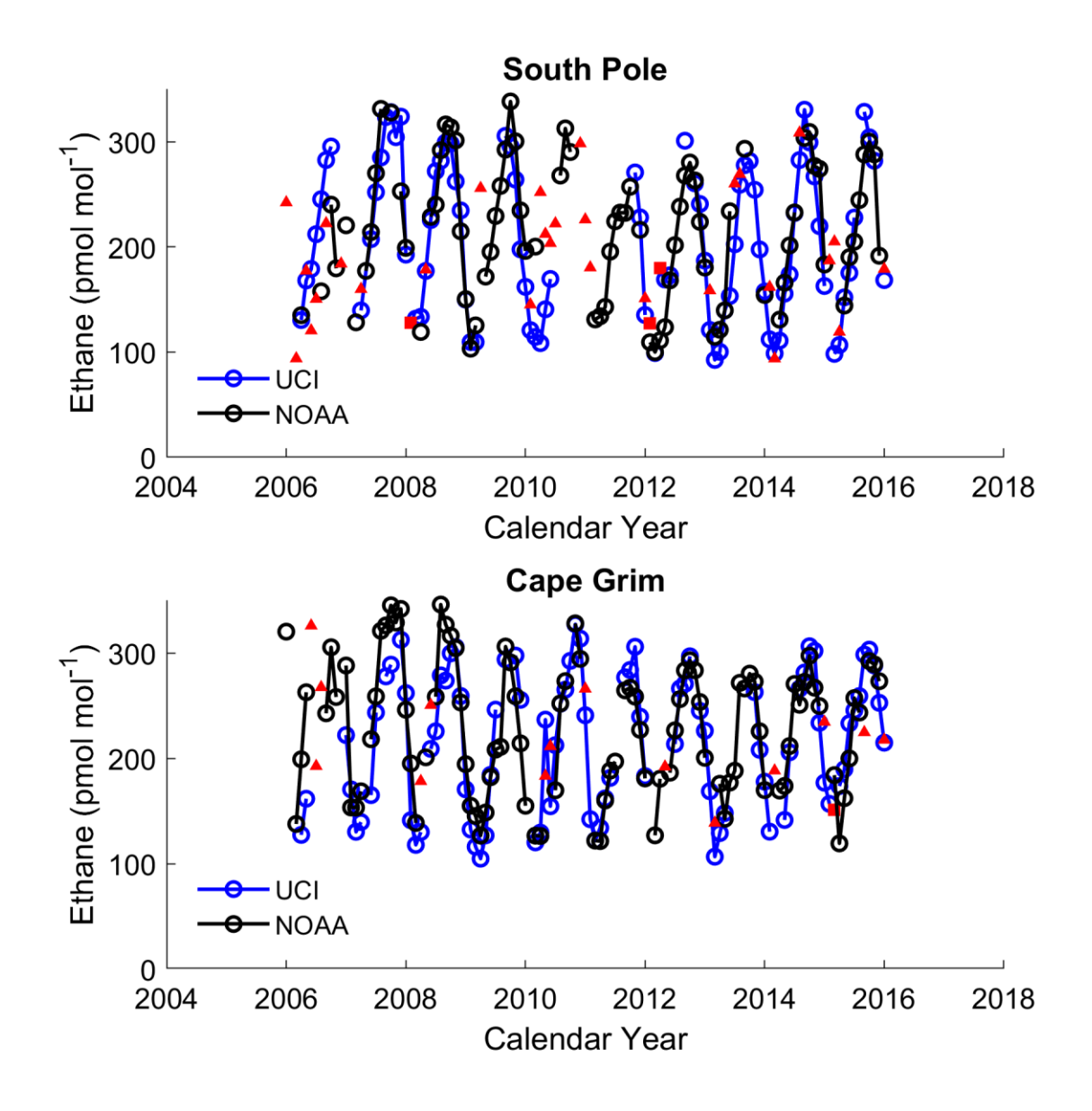
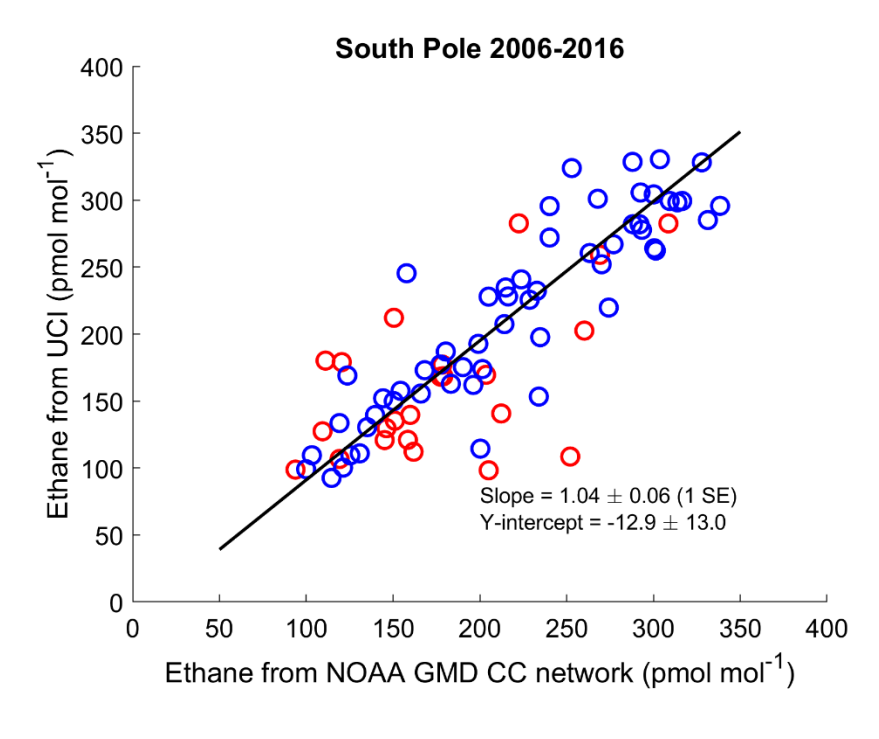


Fig. S6 Ethane surface measurements from our lab (UCI, blue) and from NOAA (Helmig lab, UC Boulder, black; ref. 16) from South Pole and Cape Grim from 2006-2016. Red markers denote UCI (red squares) and NOAA (red triangles) data excluded as part of the quality control as described in the SI text.



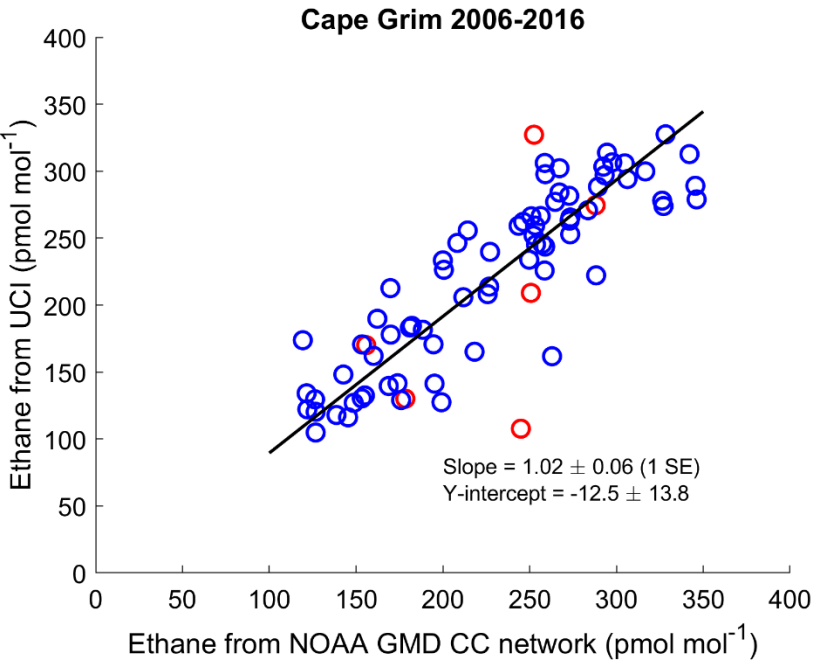


Fig. S7 Two-way regression between the UCI and NOAA ethane flask measurements for South Pole (top) and Cape Grim (bottom). The errors on the slope and y-intercept are 1 standard error. Red circles denote data that was rejected based on the quality control procedures described in the SI Appendix.

Table S1. Spatial and monthly distributions of ethane emissions used in the UCI-CTM for each source and the resulting model sensitivities for Greenland and Antarctica.

		Modeled Sensitivities	
		(pmol mol ⁻¹ /Tg y ⁻¹)	
Emissions	Spatial and monthly distribution	Greenland	Antarctica
Non-boreal biomass burning	GFED3 (ref. 20)	18.4	24.2
Boreal biomass burning (50°N-90°N)	GFED3 (ref. 20)	190.5	2.4
Biofuel burning	Yevich and Logan (ref. 21)	65.4	11.4
Geologic	Etiope and Ciccioli (ref. 22)	80.9	12.9

Table S2. Modeled ethane budget during the Medieval Period (1000-1500 CE) and the Little Ice Age (1600-1800 CE). Budgets were calculated by taking the mean of all scenarios which satisfy the cost-function for ethane (see main text). Values are reported as mean \pm 1 σ in Tg ethane y⁻¹

Geologic	Mean Boreal		Mean Non-boreal Burning	
	1000-1500 CE	1600-1800 CE	1000-1500 CE	1600-1800 CE
2	1.4 ± 0.2	1.2 ± 0.1	4.0 ± 0.3	2.5 ± 0.2
3	1.0 ± 0.2	0.8 ± 0.1	3.4 ± 0.3	2.0 ± 0.2
4	0.7 ± 0.2	0.5 ± 0.1	3.0 ± 0.3	1.6 ± 0.2

Table S3. Methane budget during the Medieval Period (1000-1500 CE) and the Little Ice Age (1600-1800 CE). Budgets were calculated by taking the mean of all scenarios which satisfy the cost-function for methane (see main text). Values are reported as mean $\pm 1\sigma$ in Tg methane y^{-1}

Geologic	Mean Microbial		Mean Biomass Burning	
	1000-1500 CE	1600-1800 CE	1000-1500 CE	1600-1800 CE
0	167.2 ± 6.0	186.2 ± 9.7	47.5 ± 1.9	42.3 ± 2.8
10	168.8 ± 10.1	182.8 ± 11.5	45.0 ± 3.1	37.7 ± 3.1
20	163.3 ± 10.0	177.4 ± 11.2	40.1 ± 3.3	32.9 ± 3.1
30	158.6 ± 10.0	172.6 ± 11.1	35.5 ± 3.1	28.1 ± 3.1
40	153.2 ± 9.8	167.3 ± 11.1	30.6 ± 3.2	23.2 ± 3.0
50	148.1 ± 10.3	162.4 ± 11.1	25.9 ± 3.3	18.5 ± 3.0
60	142.5 ± 10.0	157.5 ± 11.2	20.8 ± 3.3	13.7 ± 3.0
70	137.0 ± 10.1	151.8 ± 11.0	16.0 ± 3.3	8.7 ± 3.0

Table S4. Kinetic isotope effect (α) for methane losses used in the box model. Values are taken from Table 3 in ref. 13.

Loss	Relative Contribution (%)	$\alpha = k(^{13}CH_4)/k(^{12}CH_4)$
Troposphere (OH)	88	0.9961
Stratosphere	7	0.9847
Soils	5	0.9824

Table S5. Methane isotopic source end-member signatures used in the box model. Values are from ref. 12.

Source	δ ¹³ C (‰)	
Microbial (wetlands, agriculture)	-62.3	
Geologic/Fossil	-43.0	
Biomass burning	-22.3	
Biofuel burning	-22.3	

Table S6. Modern budget (2010 CE) for CH₄ and ethane used for Fig 4. Emissions are in units of Tg yr⁻¹.

Source	CH ₄	Ethane
Fossil fuel	185 (ref. 12)	12 (ref. 16, 25)
Biofuel	25 (ref. 23)	2.6 (ref. 25)
Geologic	60 (ref. 22)	3 (ref. 22)
Microbial	180 (ref. 12)	
Agriculture	170 (ref. 23)	
Biomass burning	21 (ref. 24)	3.4 (ref. 24)

References

- 1. Cuffey KM, Clow GD (1997) Temperature, accumulation, and ice sheet elevation in central Greenland through the last deglaical transition. *J Geophys Res* 102(C12):26383–26396.
- 2. Meese DA, et al. (1997) The Greenland Ice Sheet Project 2 depth-age scale: methods and results. *J Geophys Res* 102:26,411-26,423.
- 3. Schwander J, et al. (1997) Age scale of the air in the summit ice: Implication for glacial-interglacial temperature change. *J Geophys Res* 102:19483–19493.
- 4. Aydin M, Williams MB, Saltzman ES (2007) Feasibility of reconstructing paleoatmospheric records of selected alkanes, methyl halides, and sulfur gases from Greenland ice cores. *J Geophys Res* 112:D07312.
- 5. Souney JM, et al. (2014) Core handling and processing for the WAIS Divide ice-core project. *Ann Glaciol* 55:15–26.
- 6. Mitchell LE, Brook EJ, Sowers T, McConnell JR, Taylor K (2011) Multidecadal variability of atmospheric methane, 1000-1800 C.E. *J Geophys Res Biogeosci* 116:G02007.
- 7. Buizert C, et al. (2015) The WAIS Divide deep ice core WD2014 chronology Part 1: Methane synchronization (68-31 ka BP) and the gas age-ice age difference. *Clim Past* 11(2):153–173.
- 8. Sigl M, et al. (2016) The WAIS Divide deep ice core WD2014 chronology Part 2: Annual-layer counting (0-31 ka BP). *Clim Past* 12:769–786.
- 9. Casey KA, et al. (2014) The 1500m South Pole ice core: recovering a 40 ka environmental record. *Ann Glaciol* 55:137–146.
- 10. Nicewonger MR, Verhulst KR, Aydin M, Saltzman ES (2016) Preindustrial atmospheric ethane levels inferred from polar ice cores: A constraint on the geologic sources of atmospheric ethane and methane. *Geophys Res Lett* 43:1–8.
- 11. Craig H (1957) Isotopic standards for carbon and oxygen and correction factors for mass-spectrometric analysis of carbon dioxide. *Geochim Cosmochim Acta* 12:133–149.
- 12. Schwietzke S, et al. (2016) Upward revision of global fossil fuel methane emissions based on isotope database. *Nature* 538:88–91.
- 13. Mischler JA, et al. (2009) Carbon and hydrogen isotopic composition of methane over the last 1000 years. *Global Biogeochem Cycles* 23:GB4024.

- 14. Aydin M, et al. (2011) Recent decreases in fossil-fuel emissions of ethane and methane derived from firn air. *Nature* 476(7359):198–201.
- 15. Schultz MG, et al. (2015) The Global Atmosphere Watch reactive gases measurement network. *Elem Sci Anth* 3(December).
- 16. Helmig D, et al. (2016) Reversal of global atmospheric ethane and propane trends largely due to US oil and natural gas production. *Nat Geosci* 9(7):490–495.
- 17. Marlon JR, et al. (2008) Climate and human influences on global biomass burning over the past two millennia. *Nat Geosci* 2:307–307.
- 18. Ferretti DF, et al. (2005) Unexpected changes to the global methane budget over the past 2000 years. *Science* 309:1714–1717.
- 19. Wang Z, Chappellaz J, Park K, Mak JE (2010) Large variations in Southern Hemisphere biomass burning during the last 650 years. *Science* 330:1663–1666.
- 20. van der Werf GR, et al. (2010) Global fire emissions and the contribution of deforestation, savanna, forest, agricultural, and peat fires (1997-2009). *Atmos Chem Phys* 10:11707–11735.
- 21. Yevich R, Logan JA (2003) An assessment of biofuel use and burning of agricultural waste in the developing world. *Global Biogeochem Cycles* 17
- 22. Etiope G, Ciccioli P (2009) Earth's degassing: a missing ethane and propane source. *Science* 323:478.
- 23. Kirschke S, et al. (2013) Three decades of global methane sources and sinks. *Nat Geosci* 6(10):813–823.
- 24. van der Werf GR, et al. (2017) Global fire emissions estimates during 1997-2016. *Earth Syst Sci Data* 9(2):697–720.
- 25. Xiao Y, et al. (2008) Global budget of ethane and regional constraints on U.S. sources. *Quat Sci Rev* 113:D21306.

.